Electron-impact excitation of the second positive band system ($C\ ^3\Pi_u \rightarrow B\ ^3\Pi_g$) and the $C\ ^3\Pi_u$ electronic state of the nitrogen molecule

John T. Fons, R. Scott Schappe,* and Chun C. Lin
Department of Physics, University of Wisconsin, Madison, Wisconsin 53706
(Received 18 August 1995)

Absolute optical emission cross sections have been measured for the second-positive band system of N_2, $C\ ^3\Pi_u(v') \rightarrow B\ ^3\Pi_g(v'')$, for $v'=0,1,2,3,4$ and v'' as large as 9 produced by electron impact with the nitrogen molecule for incident-electron energies from threshold up to 600 eV. The relative cross sections for each v' family are in good agreement with the theoretical values. From the measured optical emission cross section, the apparent excitation cross sections for the $v'=0,1,2,3,4$ vibrational levels of the $C\ ^3\Pi_u$ electronic states are determined. A comparison of these apparent cross sections with the relative direct excitation cross sections predicted by the Franck-Condon principle suggests that the population of the $C\ ^3\Pi_u$ state in an electron-beam experiment for the $v'=0,1,$ and 2 levels is primarily due to direct excitation with minor contributions from cascade. For the $v'=3$ and 4 levels, the direct excitation cross sections are much smaller so that a larger percentage population is attributed to cascade. The relative intensities of the various (v',v'') bands in the electron-beam experiments are also compared with those observed in a dc discharge.

PACS number(s): 34.80.Gs, 34.50.Gb

I. INTRODUCTION

Electron excitation of the nitrogen molecule plays an important role in atmospheric phenomena and laser physics. One of the most predominant emission characteristics of the nitrogen molecule is the second positive band corresponding to the $C\ ^3\Pi_u \rightarrow B\ ^3\Pi_g$ electronic transition [1]. While the electron-impact cross sections for the various vibrational bands of the second positive systems have been measured by researchers in several laboratories [2–9], considerable discrepancies exist in the published data.

Most of the earlier measurements of the optical emission cross sections were made for $v' \leqslant 2$. In particular, the papers by Jobe, Sharpton, and St. John [3], by Burns, Simpson, and McConkey [2], and by Shaw and Campos [7] have reported cross sections for a large number of these bands. Substantial disagreement, however, is found for the cross sections given therein. The bands with $v'=3$ and 4 are much weaker and fewer measurements have been reported for these bands. A recent study of the electron-impact excitation of vibrational levels of the $C\ ^3\Pi_u$ state of N_2 suggested a significant deviation from the Franck-Condon approximation [9].

In this paper we report a comprehensive measurement of the optical emission cross sections of the (v',v'') bands of the $C\ ^3\Pi_u \rightarrow B\ ^3\Pi_g$ transitions produced by electron impact with $v'=0,1,2,3,4$; v'' as large as 9; and electron energy up to 600 eV. The results of our optical emission cross sections are compared with those from other laboratories. Since the $C \rightarrow B$ transition is the only radiative decay channel of the $C\ ^3\Pi_u$ state, summation of the optical emission cross sections of the (v',v'') bands over v'' gives the apparent electron excitation cross section of the $C\ ^3\Pi_u(v')$ vibrational level, which represents the sum of the direct excitation and the cascade into the particular vibrational level. An analysis of the apparent excitation cross sections for the various vibrational levels allows us to address the issue of deviation from the Franck-Condon approximation. The relevant electron-excitation and radiative processes are shown in Fig. 1.

The $C\ ^3\Pi_u \rightarrow B\ ^3\Pi_g$ transition moment as a function of the internuclear distance has been given in the comprehen-

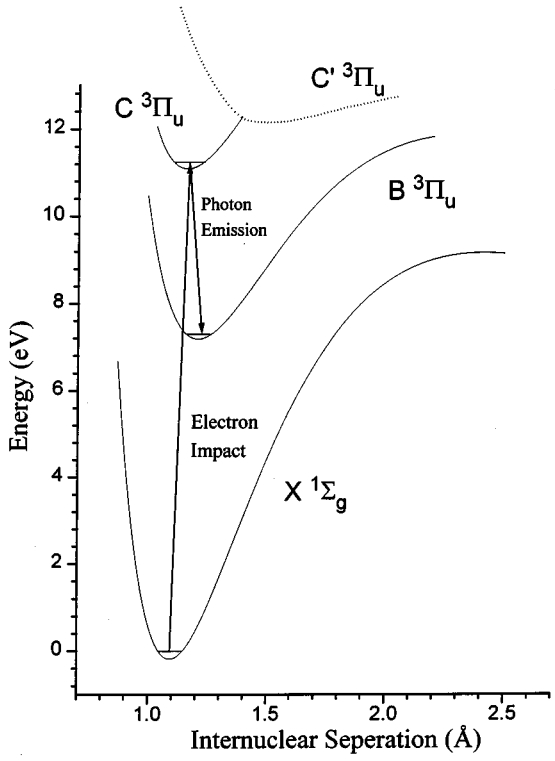

FIG. 1. Electronic energy curves of the nitrogen molecule, showing the relevant energy levels for electron-impact excitation of the second positive band system emissions.

*Present address: Department of Physics, University of South Alabama, Mobile, AL 36688.

sive work of Gilmore, Laher, and Espey [10] so that the transition matrix element connecting the $C\ ^3\Pi_u(v')$ to the $B\ ^3\Pi_g(v'')$ vibrational levels can be evaluated without resorting to the Franck-Condon approximation. If one adopts the Franck-Condon approximation, the theoretical values of the relative transition probabilities of the (v',v'') are governed entirely by the Franck-Condon factors and the wavelengths. In Sec. IV we compare the measured relative cross sections with the theoretical values of the transition probabilities calculated with and without the use of the Franck-Condon approximation.

A common way to determine the emission cross section of a weak transition is to utilize the fact that the intensity ratio of the (v',v''_a) to (v',v''_b) transitions in a discharge experiment is equal to the ratio of the respective transition rates, independent of the mechanisms of populating the upper level v', and therefore is the same as the intensity ratio observed in an electron-beam experiment [11]. Suppose in an electron-beam experiment the (v',v''_a) emission cross section is measured but the (v',v''_b) band is too weak to detect. One can then resort to a discharge where all the emission bands are much brighter than in an electron-beam experiment so that the intensities of both the (v',v''_a) and (v',v''_b) bands can be measured. This allows us to determine the (v',v''_b) cross section from the ratio relation, if one can assume that the populations of the v''_a and v''_b are sufficiently low so that the effect of photon reabsorption on the intensity ratios can be neglected. Observations of possible dependence of the intensity ratios of the (v',v''_a) to (v',v''_b) bands on the discharge conditions have been reported [12]. To examine this point, we have measured the intensity ratios for the second positive band system in a discharge under different conditions and compare the results with those of our electron-beam experiment. Our data, which cover a wide range of v'' for both the electron-beam and discharge experiments, provide a check on the relative theoretical transition probabilities and the Franck-Condon approximation.

II. EXPERIMENT

Figure 2 shows the apparatus used to measure the optical emission cross section, which is similar to the one used by Filippelli, Chung, and Lin [13]. Detailed descriptions of this apparatus can be found in Refs. [13] and [14], thus only a brief discussion of the experimental methods is given here. A series of grids that make up an electron gun electrostatically accelerates electrons produced by an indirectly heated BaO cathode. The electron beam produced is relatively monoenergetic, $\Delta E \approx 0.6$ eV, and is approximately 3 mm in diameter. The beam is collected in a Faraday cup, not shown in Fig. 2, and the magnitude of the current is continuously monitored and recorded. The end plate of the Faraday cup has been biased to 81 V, relative to the collision region, to help prevent electrons from reflecting off the base of the Faraday cup and reentering the collision region. This bias has been shown to produce a negligible electric field in the collision region [15]. The presence of reflected electrons has been monitored by the last plate of the electron gun system, adjacent to the Faraday cup. The current on this plate has shown to be negligible, less than 0.5% of the initial beam, which implies that very few reflected electrons are returning to the collision region.

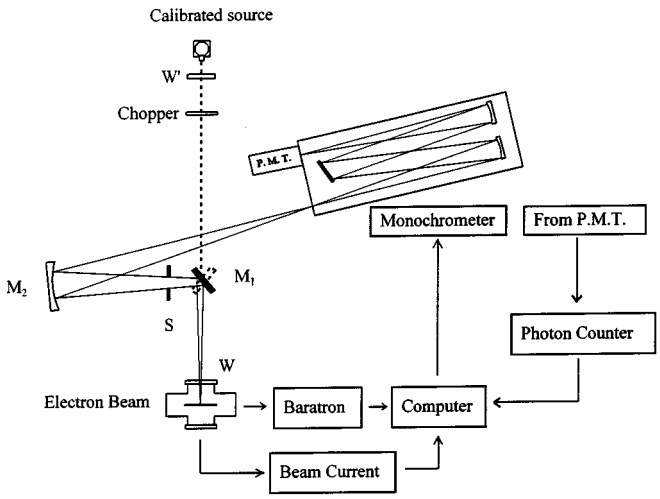

FIG. 2. Optical layout of the electron-beam experiment. M_1 is a rotatable plane mirror, M_2 is a spherical mirror, W is the uv grade quartz window on the collision chamber, W' is the compensating window, and S is the optical stop. M_1 is rotated 90° (dotted configuration) for absolute calibration.

The electron beam passes through a chamber that has been evacuated to a background pressure of 5×10^{-8} Torr and then filled to a pressure of about 4 mTorr with research grade nitrogen gas. With the use of leak valves and pumps, the nitrogen gas is allowed to slowly flow through the chamber to prevent the build up of contaminants or atomic nitrogen. Careful adjustment of the valves allows the pressure to remain very stable over many hours of continuous operation. The pressure of the gas within the chamber was continuously monitored and recorded. As the electron beam passes through the collision region, electron impact of the molecules results in excitation of the N_2 gas. The excitation can be electronic, vibrational, or rotational; however, in this work we are primarily concerned with the excitation into the vibrational-rotational levels of the $C\ ^3\Pi_u$ electronic state.

The radiation emitted by the electronically excited molecules through the $C\ ^3\Pi_u \rightarrow B\ ^3\Pi_g$ transition, the second positive band system, is monitored in order to determine the optical emission cross sections. In Fig. 2 the limiting stop S defines the solid angle that is used to collect the radiation exiting the window W and reflected by mirror M_1. Mirror M_2, a 0.50-m focal length spherical mirror coated for enhanced uv reflection, is used to focus the emitted radiation onto the entrance slit of the 1.26-m monochromator. Typically, the entrance and exit slits of the monochromator are set to give a triangular bandpass of 0.75 Å full width at half maximum, which does not allow for resolution of the rotational structure of the bands. The radiation is then detected by the photomultiplier tube (PMT) and the intensity of radiation divided by the electron-beam current and pressure is plotted as a function of wavelength. The PMT presently used is a RCA 31034 GaAs tube that has been thermoelectrically cooled to -25 °C to reduce the dark current. The area under the intensity versus wavelength curve is measured, for a given (v',v'') vibrational band of the $C\ ^3\Pi_u \rightarrow B\ ^3\Pi_g$ transition, and is proportional to the optical emission cross section.

By modulating the voltage on one of the grids in the electron gun, the electron beam can be electronically chopped at a rate of 1 kHz, which allows photon counting to be very effective. For low emission intensities, we have found that photon counting has proven to be far superior over the use of a lock-in detector or analog methods. While the electron beam is on, gate A detects the signal that consists of dark current, background radiation, and the emitted radiation from the collision region. While the electron beam is off, gate B detects the signal that consists of the dark current and the background radiation. By subtracting the number of counts in gate B from the number of counts in gate A, the radiation emitted from the collision region can be isolated from the background and dark current. Typically, 100–1000 s of continuous counting was done at each wavelength before advancing the monochromator to a new wavelength. The entire spectra of interest, around a band to be investigated, was scanned no less than five times and then averaged to allow the shape of the bands to be more clearly defined.

To determine the absolute intensity of the radiation emitted from the collision region, mirror M_1 is rotated 90° so that the radiation from a calibrated radiation source is directed into the monochromator through S and M_2, as shown in Fig. 2. Window W' is placed in the optical path of the calibrated source to compensate for the absorption and reflection by the exit window on the chamber W. Ultraviolet grade fused silica has been used for both W' and W to ensure that they have the same transmittance at all wavelengths. The light from the calibrated source is modulated by a mechanical chopper and again photon counting is utilized. Comparison of the signals from the collision chamber and from the calibrated source at various wavelengths enables us to determine the absolute emission intensities and hence the optical emission cross section of the (0,0) band. The absolute cross sections of the other (v',v'') bands are determined by measuring the intensities of the (v',v'') bands relative to the (0,0) band. For this purpose a deuterium and a tungsten coil standard lamps are used as the calibrated sources to measure the relative efficiencies of the entire optical system for the wavelength range 2000–6000 Å.

To determine the polarization of the radiation emitted from the collision region, a polarizer is placed near the entrance slit of the monochromator. The standard lamps are then used to determine the relative efficiency of the optical detection system for both the parallel and perpendicular polarizations over the wavelength range 2000–6000 Å. The relative intensity for a given (v',v'') band can then be determined for both directions of polarization.

The emissions of the second positive bands from a dc discharge tube has also been measured for comparison with the results of the electron-beam excitation experiments. The discharge tube is a quartz capillary tube approximately 6 in. long with an inner diameter of 5.0 mm. The N_2 within the tube was allowed to flow and the pressure of the N_2 was varied from 200 mTorr up to as high as 2000 mTorr. In our experiment, the dc voltage across the tube ranges from 400 V up to 1200 V and the current ranged from 2 mA up to as high as approximately 30 mA. The discharge tube was positioned along the optical axis of the standard lamp (Fig. 2) so the previous relative optical efficiency measurements could be used. The emissions from the discharge tube were reflected off the plane mirror M_1 passed through stop S and was focused by mirror M_2 onto the entrance slit of the monochromator. The monochromator was scanned over a wavelength range that contains a given (v',v'') band and the intensity versus wavelength plot was made using analog methods. Photon counting was not required due to the high intensity of the emission from the discharge tube; however, it was used to check the results of some of the low-intensity bands. After compensating for any contamination of the spectrum due to neighboring N_2 emission bands, the area under the wavelength versus intensity curve, for a given (v',v'') band, is measured and is used to determine the relative intensities of the various second positive bands in the discharge tube.

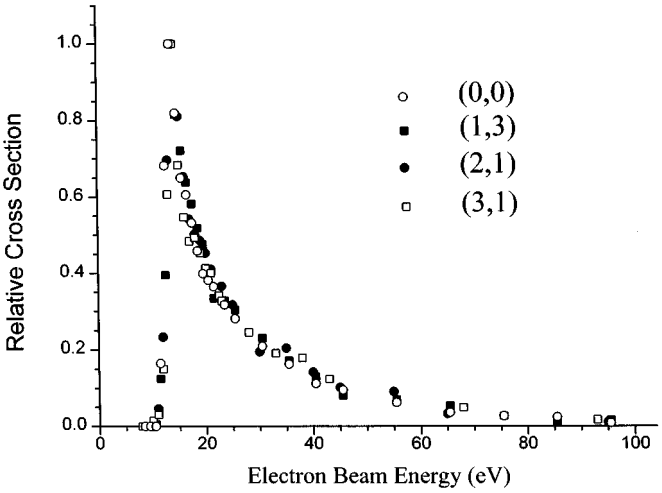

FIG. 3. Relative excitation function for the (0,0), (1,3), (2,1), and (3,1) second positive bands of N_2. The peak value is set to unity for each band.

III. RESULTS

The excitation functions of the (0,0), (1,3), (2,1), and (3,1) bands were investigated at a pressure of $\sim 5\times 10^{-4}$ Torr and the results for electron energy up to 100 eV are shown in Fig. 3. The kinetic energy of the incident electrons is not necessarily equal to the energy corresponding to the applied voltage as explained in Ref. [15]; the difference is known as the energy offset. This effect is compensated by setting the energy of the onset of the excitation function equal to the known energy difference between the initial and final states. The energy offset was found to be ~4.5 eV and for all energies reported here, compensation has been made for this difference. The general shape of the various excitation functions is quite similar, with the exception of the onset value, showing no dependence of the excitation on the vibrational quantum number v'. The energy dependence of the optical emission cross section for the (0,0) band in the range 12–600 eV is shown in Fig. 4.

In many cases, the absolute cross sections were measured at electron energies of 21 eV. Unless specified, all cross sections reported have been scaled to the peak of the excitation function. Figure 3 shows that at $E \geqslant 21$ eV, the cross section no longer varies as steeply with the energy so that uncertainty in the electron energy due to a small change in the

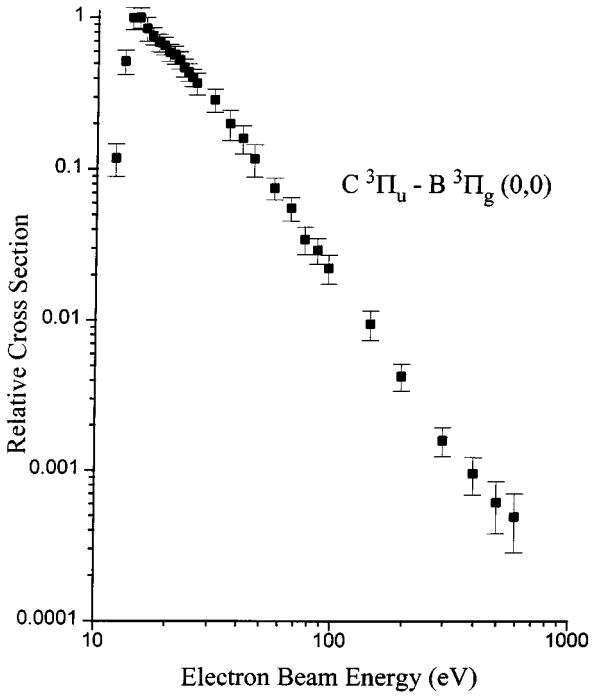

FIG. 4. Relative excitation cross section for the $C\ ^3\Pi_u \rightarrow B\ ^3\Pi_g$ (0,0) band for energies from threshold to 600 eV. The error bars represent the total uncertainty including both the statistical and systematic types.

energy offset would not cause a significant error in the absolute calibration. The energy offset was monitored regularly and any change in the offset was compensated, although it should be noted the change in the energy offset over a 4-month period was ~0.25 eV.

Some of the second positive bands are overlapped by other N_2 or N_2^+ emission bands. The first negative band system of N_2^+ ($B\ ^2\Sigma_u^+ - X\ ^2\Sigma_g^+$), for example, contaminates a number of the measured second positive bands at higher energies. To eliminate this contamination and other N_2^+ contaminating bands, the electron energy at which the absolute cross sections were measured was reduced from 21 to 19 eV, which were below or very near the onset of most N_2^+ bands [14]. This would also increase the signal from the second positive system, thus making the N_2^+ contamination even more negligible. To remove extraneous signals that have a similar onset as the second positive bands, such as the Gaydon-Herman band system ($^1\Sigma_u^+ \rightarrow a\ ^1\Pi_g$) or any other interfering N_2^+ bands, a visual extrapolation of the spectral shape of the bands was taken and the area under the intensity versus wavelength plot was adjusted accordingly [16].

The dependence on the electron-beam current and target pressure of the intensity of the (0,0) band was examined and the results are shown in Figs. 5 and 6, respectively. It can be seen that the intensity of the signal has a linear dependence on the electron-beam current, but shows a definite nonlinear dependence on the pressure at values above 2 mTorr and electron-beam energies over 100 eV. The pressure dependence is probably due to electrons undergoing multiple collisions at higher pressure and/or N_2 collisions with electrons produced in the formation of N_2^+. The ionization cross sections have been shown to typically peak above 100 eV, but

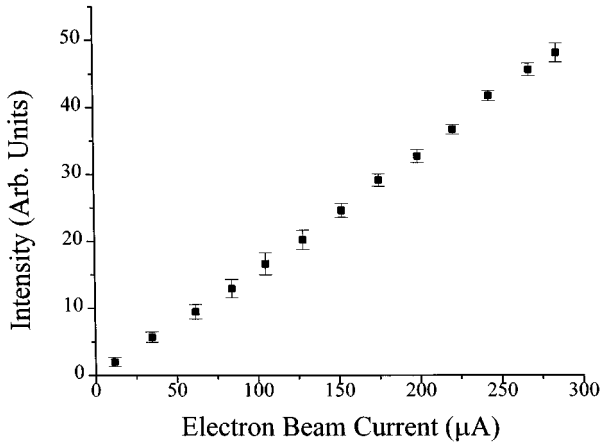

FIG. 5. Emission intensity as a function of electron beam current for the $C\ ^3\Pi_u \rightarrow B\ ^3\Pi_g$ (0,0) band. The error bars represent the total uncertainty.

remain relatively large at higher energies even above 200 eV [14,17].

The optical emission cross sections that we measured in this study are listed in Table I. The estimated uncertainty for each cross section is also given. The uncertainty of the (0,0) band is 13%, but for many other bands, the uncertainty is in the neighborhood of 20%. For a few cases of the very weak bands, the uncertainty becomes even larger. The largest source of error in the data analysis arises from the determination of the area of the intensity versus wavelength curve. The statistical and experimental uncertainties in this area measurement combine to give approximately 10–13 % error for intense bands with no contamination and up to approximately 18–20 % for weaker bands with little or no contamination. Bands that appeared to be contaminated typically had an additional uncertainty of 5–15 % due to extrapolation of the contaminating band. The standard lamp and the determi-

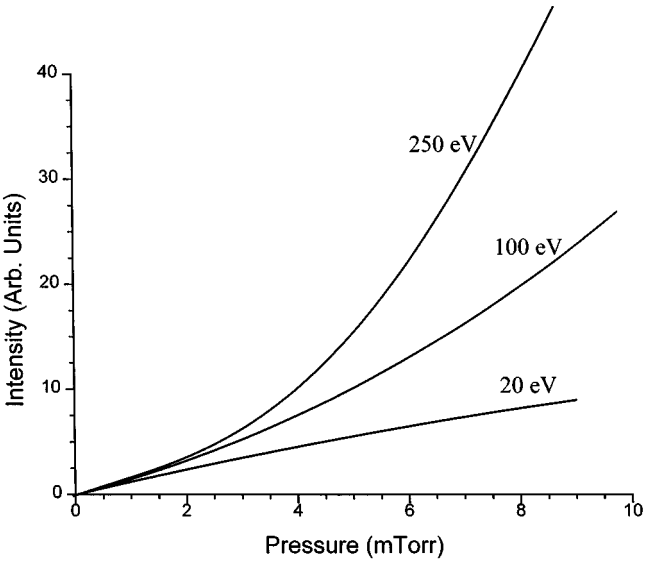

FIG. 6. Emission intensity as a function of N_2 pressure for the $C\ ^3\Pi_u \rightarrow B\ ^3\Pi_g$ (0,0) band for electron beam energies of 20, 100, and 250 eV.

TABLE I. Optical emission cross sections for the second positive band system $C\ ^3\Pi_u(v')\rightarrow B\ ^3\Pi_g(v'')$ (in units of 10^{-18} cm^2) at incident electron energies corresponding to the peak of the excitation functions. The numbers in parentheses are the uncertainty in the cross sections.

v''	$v'=0$	$v'=1$	$v'=2$	$v'=3$	$v'=4$
0	10.9 (1.4)	7.03 (1.2)	0.93 (0.16)	0.036 (0.01)	
1	6.87 (1.17)	0.30 (0.054)	2.32 (0.39)	0.50 (0.12)	0.060 (0.012)
2	2.73 (0.46)	3.16 (0.63)	0.17 (0.040)	0.41 (0.078)	0.37 (0.12)
3	0.88 (0.18)	3.02 (0.51)	0.32 (0.062)	0.20 (0.040)	0.12 (0.02)
4	0.23 (0.050)	1.12 (0.23)	0.88 (0.16)		0.096 (0.028)
5	0.042 (0.011)	0.35 (0.079)	0.58 (0.10)	0.16 (0.030)	
6		0.15 (0.031)	0.21 (0.041)	0.17 (0.032)	0.030 (0.007)
7		0.032 (0.010)	0.13 (0.030)	0.13 (0.023)	0.054 (0.014)
8			0.034 (0.007)	0.055 (0.011)	0.041 (0.01)
9				0.024 (0.005)	0.018 (0.007)

nation of the relative efficiency of the optics and detector introduced uncertainties generally less than 5%. The remaining experimental and statistical uncertainties for measuring other quantities are smaller and have been included in all reported values. The cross sections reported here are the values at the peak of the excitation function; the measured cross sections at all energies have been scaled using the excitation functions given in Fig. 3 with allowance for the slightly different onset for different v' levels.

Since the $C\rightarrow B$ transition is the only channel for radiative decay from the N_2 ($C\ ^3\Pi_u$) state, the apparent cross section $Q_{\rm app}$ for excitation into a given vibrational level (v') of the $C\ ^3\Pi_u$ electronic state can be obtained by summing the optical emission cross sections $Q(v',v'')$ of the second positive bands over v'' for a given v', i.e.,

$$Q_{\rm app}(Cv')=\sum_{v''} Q(v',v''). \tag{1}$$

The apparent cross sections is the sum of the direct cross section into the Cv' level and the cascade from higher levels. For each v' the $Q(v',v'')$ cross sections not reported in Table I have been estimated by using the Franck-Condon factors. However, the contribution from these missing optical emission cross sections to the apparent cross sections is no more than 1% for $v'=0,1,2$, no more than 4.5% for $v'=3$, and approximately 10% for $v'=4$. The apparent cross sections so obtained are given in Table II.

TABLE II. Apparent excitation cross sections (in units of 10^{-18} cm^2) for the $C\ ^3\Pi_u(v')$ vibrational levels, $Q_{\rm app}$ (Cv'), at incident energies corresponding to the peak of the excitation functions. The relative values of these cross sections in the third column are compared to the relative Franck-Condon (FC) factors. The last column gives the relative total emission rate from the $C\ ^3\Pi_u(v')$ level in a discharge, $I_{\rm dis}(Cv')$, as defined in Eq. (7).

v'	$Q_{\rm app}(Cv')$	Relative $Q_{\rm app}(Cv')$	Relative FC factors	Relative $I_{\rm dis}(Cv')$
0	21.7	1.00	1.00	1.00
1	15.2	0.70	0.57	0.64
2	5.57	0.26	0.19	0.29
3	1.76	0.081	0.055	0.27
4	0.88	0.041	0.014	0.19

The polarization of the radiation was investigated on four of the second positive bands (0,0), (1,0), (2,1), and (3,1) and at various electron beam energies 15, 21, 50, 100, and 500 eV. The magnitude of the polarization, as defined in Ref. [15], was found to be typically less than 0.04 for all four bands and five energies.

IV. DISCUSSION

A. Energy dependence of the cross section

Most of the excitation functions of the (0,0) band that have been previously reported show significant discrepancy from our data in the relative values for energies above approximately 50 eV. The excitation functions published in Refs. [2–4,7] do not decrease as quickly as ours for energies above 30 eV. If we compare the relative excitation functions reported by different groups, normalizing the peak value to unity in each case, the results of Refs. [2–4,7] at 90 eV are nearly a factor of 4 larger than our results. The excitation functions shown in [2,3,7] have been investigated at pressures typically above 1 mTorr, whereas the present results were obtained at pressures below 0.5 mTorr. Upon repeating the present investigation at a pressure of 4.0 mTorr, it was found that the excitation function more closely resembles the results of Refs. [2–4,7]. At energies of at least 100 eV and pressures greater than 1.0 mTorr, as shown in Fig. 6, the intensity of the second positive band emissions begins to exhibit a nonlinear dependence on pressure. The nonlinear pressure dependence of the emission intensity at high energy causes the tail of the excitation function to be artificially raised. Shemansky and Broadfoot [8] have given the excitation function of the second positive (0,0) band up to 50 eV. Their excitation function does not decrease as quickly as ours.

Other notable excitation functions have been reported by Aarts and De Heer [5] and by Imami and Borst [6]. The normalized excitation functions given in Refs. [5,6] are very similar to each other and show a closer resemblance to our data than do the results of Refs. [2–4,7,8]. The results of Ref. [5] have been obtained at pressures less than 1.0 mTorr and Imami and Borst [6] have studied the excitation function

at pressures less than 0.5 mTorr.

The optical emission cross section for electron-impact excitation of the $D\ ^3\Sigma_u^+ \rightarrow B\ ^3\Pi_g$ (0,1) band of N_2, reported in Ref. [13], shows an inverse-cubic energy dependence $Q \propto E^{-3.0}$, above 60 eV as expected on a Born-Ochkur-type theoretical consideration for excitation from a singlet ground state to a triplet electronic state [18]. This inverse cubic relation, however, is not seen in our cross section data for the second positive band (Fig. 4), which corresponds approximately to an energy dependence of approximately $E^{-2.3}$ at high energies. We have repeated the measurement of the excitation function at lower pressures (0.25 mTorr) and have found no change in the energy dependence. Imami and Borst [6] reported a cross-section energy dependence like $E^{-2.2}$ for their data between 20 and 200 eV, but the magnitude of the exponent decreases as the energy increases. Likewise, Aarts and De Heer [6] estimated that the cross section has an energy dependence like $E^{-1.7}$. Imami and Borst [5] have indicated the possibility of admixture of a singlet component to the wave function of the $C\ ^3\Pi_u$ state, so that the cross section does not decrease as strongly with energy as for a pure triplet state. Observations of the Tanaka system ($C\ ^3\Pi_u \rightarrow X\ ^1\Sigma_g^+$) in absorption [1] indeed suggest singlet mixture to the $C\ ^3\Pi_u$ state. However, our data show an energy dependence of $E^{-2.3}$ from 30 to 600 eV. The singlet-triplet mixing is unlikely to explain the deviation from the $E^{-3.0}$ dependence because if the singlet-triplet mixing is large enough to affect the energy dependence at 30 eV, one would expect the singlet component of the wave function to play a more dominant role on the excitation function at 600 eV, pushing more closely to the characteristic $E^{-1}\ \ln(E)$ or E^{-1} dependence for singlet states. We also believe that the energy dependence of the (0,0) band is not influenced much by cascades because this band has large cross sections and because cascades from the higher triplet states are expected to have the same kind of energy dependence as the (0,0) band itself. Since the $E^{-3.0}$ dependence was derived by use of the Ochkur approximation, it is possible that the $E^{-3.0}$ rule does not have as strong of a theoretical foundation as compared to the Born-Bethe theory and is not as universally applicable. Extensive measurements on triplet excitation cross sections at high energies for other atomic and molecular systems should prove interesting.

B. Relative emission cross sections

It is well known that the ratio of the emission cross sections for two transitions with a common upper level is equal to the ratio of the respective Einstein coefficients [15], i.e., for our case

$$\frac{Q(v',v_a'')}{Q(v',v_b'')} = \frac{A(Cv' \rightarrow Bv_a'')}{A(Cv' \rightarrow Bv_b'')}, \tag{2}$$

where A is the Einstein coefficient for the transition within the parentheses. If we use the Franck-Condon approximation, neglecting the dependence of the $C \rightarrow B$ transition moment on the internuclear distance of the N_2 molecule, the above equation becomes

$$\frac{Q(v',v_a'')}{Q(v',v_b'')} = \left[\frac{\lambda(Cv' \rightarrow Bv_b'')}{\lambda(Cv' \rightarrow Bv_a'')}\right]^3 \frac{q(Cv' \rightarrow Bv_a'')}{q(Cv' \rightarrow Bv_b'')}, \tag{3}$$

where λ is the wavelength and q is the Franck-Condon factor for the transition inside the parentheses. The optical emission cross sections summarized in Table I allow us to compare our experimental results with theory according to Eq. (2) and its approximate version Eq. (3). In Table III, we group together the transitions for each v' with various v'' and list the relative cross sections within each group, setting the largest cross section to unity. The values of the Einstein coefficients and Franck-Condon factors used in the third and fourth columns are taken from the work of Gilmore, Laher, and Espy [10].

Generally the measured cross sections show good overall agreement with theoretical values based on both Eqs. (2) and (3). Where there is significant difference between the two sets of theoretical values in Table III, the present results, in most cases, tend to match more closely the predictions of the more exact expression, Eq. (2), except for the case of $v'=4$. In the few cases of $v'=4$ and $v''=4,6,7,8,9$, where the experimental data appear to be closer to the calculations based on the approximate theory of Eq. (3) than those based on the exact theory of Eq. (2), this anomaly may be attributed to the uncertainty in the transition moment used to calculate the transition probabilities in Eq. (2). The $C \rightarrow B$ transition moment function shown in Ref. [10] was obtained by fitting the theoretical values of the transition moments calculated by Werner, Kalcher, and Reinsch [19] for five internuclear distances between 0.95 and 1.4 Å to a Gaussian function. Werner, Kalcher, and Reinsch [19] indicate that their calculated lifetimes for the $v'=3$ and 4 levels of $C\ ^3\Pi_u$ somewhat depend on the values of the transition moment at the internuclear distances of 1.4 Å, which is in the region where the C and C' states interact strongly. In this region, as pointed out in Ref. [19], in order to obtain reliable transition moments, the relative weights of the C and C' states must be accurately reproduced. Thus the transition probabilities calculated by using the $C \rightarrow B$ transition moments of Ref. [19] are less reliable for the higher vibrational states than for the lower states, which have negligible amplitude in the region where the C and C' states interact significantly.

Of the previous works cited earlier, measurements of the (v',v'') emission cross sections with $v'=0,1,2$ and numerous values of v'' have been reported by Jobe, Sharpton, and St. John [3], by Burns, Simpson, and McConkey [2], and by Shaw and Campos [7]. The relative cross sections from these three papers are included in Table III. In general, our relative cross sections are much closer to the results of Refs. [2,7] than those of Ref. [3] As to the absolute values, our peak cross sections of $(10.9\pm1.4)\times10^{-18}$, $(7.03\pm1.20)\times10^{-18}$, and $(2.32\pm0.39)\times10^{-18}$ cm^2, respectively, for the (0,0), (1,0), and (2,1) can be compared to the corresponding values of 10.8×10^{-18}, 8.6×10^{-18}, and 3.2×10^{-18} cm^2 from Ref. [3]; 11.8×10^{-18}, 6.5×10^{-18}, and 1.90×10^{-18} cm^2 from Ref. [2]; and 11.9×10^{-18}, 8.72×10^{-18}, and 2.90×10^{-18} cm^2 from Ref. [7]. For absolute cross sections with $v'>2$, we have found only the work of Stewart and Gabathuler [4], which covers the (3,3), (3,5), and (4,4) bands. Their reported values at 35 eV are about 90–170 % higher than ours at the

TABLE III. Relative optical emission cross sections for each (v',v'') series of the same v'.The second through sixth columns give the results of the present work, the theoretical values according to Eq. (2), the theoretical values according to Eq. (3), the experimental values of Jobe, Sharpton, and St. John, the experimental values of Burns, Simpson, and McConkey, and the experimental values of Shaw and Campos. The last column shows the relative optical emission cross sections measured in a discharge tube based on Eq. (4).

Band	Present results	Theory Eq. (2)	Theory Eq. (3)	Jobe *et al.* [3]	Burns *et al.* [2]	Shaw and Campos [7]	Discharge tube
(0,0)	1.00	1.00	1.00	1.00	1.00	1.00	1.00
(0,1)	0.63	0.67	0.60	0.79	0.64	0.64	0.63
(0,2)	0.25	0.27	0.22	0.41	0.23	0.24	0.27
(0,3)	0.081	0.082	0.065	0.11	0.10	0.071	0.081
(0,4)	0.021	0.022	0.016	0.031	0.016	0.017	0.020
(0,5)	0.0039	0.0053	0.0037	0.011		0.059	0.0035
(0,6)		0.0012	0.00081				0.0009
(1,0)	1.00	1.00	1.00	1.00	1.00	1.00	1.00
(1,1)	0.043	0.049	0.049	0.058	0.054	0.047	0.046
(1,2)	0.45	0.47	0.47	0.36	0.44	0.38	0.47
(1,3)	0.43	0.41	0.41	0.36	0.40	0.26	0.39
(1,4)	0.16	0.20	0.20	0.26	0.22	0.14	0.18
(1,5)	0.050	0.075	0.048	0.070	0.075	0.058	0.067
(1,6)	0.021	0.023	0.023	0.030	0.016	0.016	0.020
(1,7)	0.0045	0.0065	0.0038	0.014		0.0061	0.005
(2,0)	0.40	0.39	0.45	0.34	0.41	0.48	0.52
(2,1)	1.00	1.00	1.00	1.00	1.00	1.00	1.00
(2,2)	0.073	0.079	0.059	0.063	0.095	0.079	0.088
(2,3)	0.14	0.17	0.13	0.11	0.15	0.14	0.20
(2,4)	0.38	0.40	0.28	0.31	0.39	0.29	0.42
(2,5)	0.25	0.31	0.20	0.31	0.20	0.27	0.24
(2,6)	0.091	0.16	0.096	0.14	0.14	0.12	0.11
(2,7)	0.055	0.061	0.036	0.066	0.049	0.048	0.059
(2,8)	0.015	0.020	0.012	0.044		0.022	0.023
(3,0)	0.072	0.072	0.092				0.076
(3,1)	1.00	1.00	1.00				1.00
(3,2)	0.82	0.81	0.72				0.84
(3,3)	0.40	0.39	0.28				0.33
(3,4)		0.016	0.012				0.01
(3,5)	0.32	0.32	0.19				0.33
(3,6)	0.34	0.41	0.23				0.30
(3,7)	0.25	0.28	0.14				0.20
(3,8)	0.11	0.13	0.066				0.10
(3,9)	0.048	0.054	0.025				0.04
(4,0)		0.002	0.004				
(4,1)	0.16	0.14	0.19				0.13
(4,2)	1.00	1.00	1.00				1.00
(4,3)	0.32	0.33	0.31				0.28
(4,4)	0.26	0.41	0.26				0.30
(4,5)		0.014	0.007				0.010
(4,6)	0.081	0.11	0.065				0.074
(4,7)	0.15	0.26	0.14				0.12
(4,8)	0.13	0.23	0.11				0.14
(4,9)	0.05	0.14	0.064				0.055

same energy. Hirabayashi and Ichimura [9] have measured the emission cross sections of the (3,2) and the (4,2) bands relative to the (0,0) band, but no absolute cross sections were reported.

C. Relative emission intensities in a dc discharge

Let us consider, in place of the electron-beam excitation experiment, a nitrogen discharge and its radiation associated with the $Cv' \rightarrow Bv''$ transitions. Here the population of a

particular level Cv' is generally due to a combination of several mechanisms rather than electron-impact excitation alone as in the electron-beam experiment. The intensity ratios of the $Cv' \rightarrow Bv''_a$ and $Cv' \rightarrow Bv''_b$ transitions is equal to the ratios of the respective emission rates, independent of the mechanism for populating the Cv' level. If the number density of the N_2 molecules in the Bv'' level is sufficiently low so that one can neglect the reabsorption of the $Cv' \rightarrow Bv''$ emission, then the $Cv' \rightarrow Bv''$ emission rate can be taken as the ratios of the Einstein A coefficients

$$\frac{I_{\rm dis}(Cv' \rightarrow Bv''_a)}{I_{\rm dis}(Cv' \rightarrow Bv''_b)} = \frac{A(Cv' \rightarrow Bv''_b)}{A(Cv' \rightarrow Bv''_b)} = \frac{Q(Cv' \rightarrow Bv''_b)}{Q(Cv' \rightarrow Bv''_b)}, \tag{4}$$

where $I_{\rm dis}$ refers to the photon emission rates observed in a discharge. Equation (4) furnishes a simple means to measure the optical cross sections for some weak emission bands. As mentioned in the Introduction, a very small $Cv' \rightarrow Bv''_b$ optical emission cross section can then be obtained from the appropriate intensity ratio measured in a discharge along with the $Q(Cv' \rightarrow Bv''_a)$ measured in the electron-beam experiment in accordance with Eq. (4). However, Tyte [12] has reported the relative intensities of the (v',v'') bands of the N_2 second positive system originating from the same v' level and found the relative intensities to vary with the discharge conditions. Their results therefore raise some question about the procedure of using relative intensities measured in a discharge to determine the emission cross sections of weak bands.

To investigate this point, we have measured the relative photon emission rates for each (v',v'') series with a given v' in a discharge. The results obtained by operating the discharge at a pressure (N_2) of 380 mTorr and a current of 7 mA are shown in the last column of Table III. The agreement between the relative intensities observed in the discharge and in our collision chamber experiment is remarkably good. Under our experimental conditions, the signal from the discharge tube is typically about 50 times stronger than in the collision chamber. We have monitored the relative intensities of selected bands as we increase the N_2 pressure up to 2000 mTorr and current up to 30 mA and found no change within the experimental uncertainty. At these extreme conditions, the signal from the discharge is typically about 500 times brighter than in the collision chamber.

It is difficult to make a quantitative comparison of our measurements with those of Tyte because of the difference in the discharge tubes. Tyte's measurements cover a wider range of current density, but his data points show much scatter around a straight line plot of the intensity ratio versus the logarithm of the current density. Nevertheless, our experiment demonstrates the constancy of the intensity ratio in Eq. (4) independent of the discharge parameters within a wide range of current densities and gas pressures and thus verifies the validity of using Eq. (4) to obtain relative cross sections. However, if the discharge produces a significant quantity of molecules in the lower levels of the transitions so that reabsorption is not negligible, the intensity ratio observed in the discharge may not be equal to the ratio of the Einstein coefficients. In such measurements, it is important to monitor the observed intensity ratio to ensure that they are independent of the discharge parameters.

D. Apparent cross sections for the $C\ ^3\Pi_u(v')$ levels

The apparent cross sections for electron excitation into a level is equal to the direct cross section plus the total cascade into that level from all the higher levels, i.e.,

$$Q_{\rm app}(Cv') = Q_{\rm dir}(Cv') + \sum_{K,v} Q(Kv \rightarrow Cv'), \tag{5}$$

where Kv represents any upper lying level that decays to the $C\ ^3\Pi_u$ level. An example of the cascading state is $E\ ^3\Sigma_g^+$, which is about 1 eV above $C\ ^3\Pi_u$.

Under the Franck-Condon approximation, the direct excitation cross section for the various vibrational levels of the C state are related to the Franck-Condon factors between the initial and final levels involved in the transitions as

$$\frac{Q_{\rm dir}(Cv'_a)}{Q_{\rm dir}(Cv'_b)} = \frac{q(X0 \rightarrow Cv'_a)}{q(X0 \rightarrow Cv'_b)}, \tag{6}$$

where $X0$ stands for the ground electronic-vibrational state $X\ ^1\Sigma_g^+(v=0)$. If the cascade is assumed to be small in comparison with the direct excitation cross section, we can compare the apparent excitation cross section with the appropriate Franck-Condon factors. The relative values of the apparent cross section and of the Franck-Condon factors as shown in Table II agree rather well for $v'=0$, 1, and 2 and the difference may be attributed to cascade. From $v'=2$ to 3 an abrupt decrease both in relative Franck-Condon factor (or the direct excitation cross section) and in the relative apparent cross section can be seen. Cascade from the higher electronic states into the various $C(v')$ vibrational levels are not expected to show the same kind of abrupt change from $v'=2$ to 3 because this abrupt change is the result of the Franck-Condon factors between the $X\ ^1\Sigma_g^+$ and the $C\ ^3\Pi_u$ states. If the cascade into the $C(v')$ vibrational levels has a more even variation with v', then the $v'=3$ and 4 states should have a higher percentage cascade contribution to the apparent excitation cross sections than do the $v'=0$, 1, and 2 states because of the smaller direct excitation cross sections of the former group. This explains the larger percentage difference between the relative apparent cross section and relative Franck-Condon factors in Table II for $v'=3$ and 4 compared to $v'=0,1,2$. In this regard our findings are quite different from those of Hirabayashi and Ichimura [9]. Our relative cross sections in Table II show less deviation from the Franck-Condon factors in going from $v'=1$ and 2 to $v'=3$ than the data in Ref. [9]. Also the data in Ref. [9] indicates that the $v'=3$ cross section is more than five times larger than the $v'=4$ cross section, whereas we find only a factor of 2 for the same ratio in our experiment. We believe that the deviation of the apparent excitation cross sections from the Franck-Condon relation is consistent with the cascade description and does not necessarily signify a breakdown of the Franck-Condon picture. In the case of a discharge, the population of the Cv' levels are due to direct excitation as well as other more complicated mechanisms and are therefore not expected to show a correlation with the Franck-Condon factors in Table II. To illustrate this, we define the total emission rate from the Cv' level in a discharge as

$$I_{\rm dis}(Cv')=\sum_{v''} I_{\rm dis}(Cv'\rightarrow Bv''), \tag{7}$$

analogous to the apparent excitation cross section in Eq. (1), and list the relative values of $I_{\rm dis}(Cv')$ in Table II. Here the emission intensities from the $v'=3$ and 4 levels are rather close to that of the $v'=2$ level, in contrast to the results of the electron-beam experiment. This indicates that the $v'=3$ and 4 levels are populated primarily by processes other than electron impact excitation. On the other hand, the relative total emission rates for the $v'=0,1,2$ observed in the discharge track very closely to the results of the electron-beam experiment. In other words, the discharge and electron-beam experiments show nearly the same relative population for the $v'=0$, 1, and 2 levels of the $C\ ^3\Pi_u$ state. Information of this kind is useful toward understanding the detailed mechanisms for populating the excited electronic states in a discharge.

V. SUMMARY AND CONCLUSIONS

We have measured the optical emission cross sections for electron-impact excitation of the (v',v'') vibrational bands of the second positive system of the N_2 molecule for $v'=0,1,2,3,4$; v'' as large as 9; and electron energies up to 600 eV. The emission cross section for the (0,0) band shows an energy dependence of $E^{-2.3}$ for electron energies from 60 to 600 eV. Since the cascade population into the $C\ ^3\Pi_u(v'=1)$ level is small, the observed $E^{-2.3}$ relation also closely represents the energy dependence of the direct excitation cross section and differs from the $E^{-3.0}$ dependence for excitation from a singlet to a triplet electronic transitions found in other systems.

Except for some of the bands with $v'=4$, the ratio of the cross sections for the (v',v''_a) to the (v',v''_b) bands are in excellent agreement with the theoretical Einstein coefficients calculated using a transition moment function that depends on the internuclear distance. The larger discrepancy for the $v'=4$ bands may be due to the interaction between the $C\ ^3\Pi_u$ and $C'\ ^3\Pi_u$ states, which has not been taken into account in the calculations of the transition moments.

We have also measured the emission intensities of the (v',v'') bands observed in a gas discharge with pressures ranging from 200 mTorr up to 2000 mTorr and current of 2 mA up to 30 mA. The intensity ratio of two emission bands originating from the same upper state, i.e., (v',v''_a) and (v',v''_b), is found to be independent of the gas discharge condition and equal to the ratio observed in the electron-beam experiment, as one would expect if secondary processes such as reabsorption of the second positive band emissions are absent. These results confirm the validity of using the intensity ratio observed in a discharge to determine the optical emission cross sections of weak bands.

We have determined the apparent excitation cross sections for the $C\ ^3\Pi_u(v')$ electronic-vibrational levels for $v'=0,1,2,3,4$. Since the direct excitation cross sections are proportional to the Franck-Condon factors connecting $C\ ^3\Pi_u(v')$ to the ground vibrational level of the ground electronic state $X\ ^1\Sigma_g(0)$, we compare our relative apparent excitation cross sections with these Franck-Condon factors. Reasonably good agreement is found for $v'=0,1,2$, indicating that cascade makes only a minor contribution to the population of these levels. The discrepancy is much larger for the $v'=3$ and 4 levels. This is explained on the basis that the direct excitation cross sections for the $v'=3,4$ levels are much smaller than those for the $v'=0,1,2$ levels because of the unfavorable Franck-Condon factors resulting in a much larger percentage contribution from the other populating mechanisms such as cascade.

ACKNOWLEDGMENT

This work was supported by the U.S. Air Force Office of Scientific Research.

[1] A. Lofthus and P. H. Krupenie, J. Chem. Ref. Data **6**, 113 (1977).
[2] D. J. Burns, F. R. Simpson, and J. W. McConkey, J. Phys. B **2**, 52 (1969).
[3] J. D. Jobe, F. A. Sharpton, and R. M. St. John, J. Opt. Soc. Am. **57**, 106 (1967).
[4] D. T. Stewart and E. Gabathuler, Proc. Phys. Soc. London **72**, 287 (1958).
[5] J. F. M. Aarts and F. J. De Heer, Chem. Phys. Lett. **4**, 116 (1969).
[6] M. Imami and W. L. Borst, J. Chem. Phys. **61**, 1115 (1974).
[7] M. Shaw and J. Campos, J. Quant. Spectrosc. Radiat. Transfer **30**, 73 (1983).
[8] D. E. Shemansky and A. L. Broadfoot, J. Quant. Spectrosc. Radiat. Transfer **11**, 1401 (1971).
[9] A. Hirabayashi and A. Ichimura, J. Phys. Soc. Jpn. **60**, 862 (1991).
[10] F. R. Gilmore, R. R. Laher, and P. J. Espey, J. Phys. Chem. Ref. Data **21**, 1005 (1992).
[11] See, for example, R. S. Schappe, M. B. Schulman, F. A. Sharpton, and C. C. Lin, Phys. Rev. A **38**, 4537 (1988).
[12] D. C. Tyte, J. Quant. Spectrosc. Radiat. Transfer **5**, 545 (1965).
[13] A. R. Filippelli, S. Chung, and C. C. Lin, Phys. Rev. A **29**, 1709 (1984).
[14] J. T. Fons, J. S. Allen, and R. S. Schappe, and C. C. Lin, Phys. Rev. A **49**, 927 (1994).
[15] A. R. Filippelli, C. C. Lin, L. W. Anderson, and J. W. Mc Conkey, Adv. At. Mol. Opt. Phys. **33**, 1 (1994).
[16] J. S. Allen, S. Chung, and C. C. Lin, Phys. Rev. A **41**, 1324 (1990).
[17] Y. Itakawa, M. Hayashi, A. Ichimura, K. Onda, K. Sakimoto, K. Takayanagi, M. Nakamura, H. Nishimura, and T. Takayanagi, J. Phys. Chem. Ref. Data **15**, 985 (1986).
[18] See, for example, B. L. Moiseiwitsch and S. J Smith, Rev. Mod. Phys. **40**, 238 (1968).
[19] H. J. Werner, J. Kalcher, and E. A. Reinsch, J. Chem. Phys. **81**, 2420 (1984).